Redox-Dependent p K a of Cu B Histidine Ligand in Cytochrome c Oxidase

ARTICLE *in* THE JOURNAL OF PHYSICAL CHEMISTRY B · NOVEMBER 2004

Impact Factor: 3.3 · DOI: 10.1021/jp0467797

Redox-Dependent pK_a of Cu_B Histidine Ligand in Cytochrome *c* Oxidase

Jason Quenneville, Dragan M. Popović, and Alexei A. Stuchebrukhov*

Department of Chemistry, University of California, One Shields Avenue, Davis, California 95616

Received: July 20, 2004; In Final Form: August 6, 2004

Cytochrome *c* oxidase is a redox-driven proton pump that converts atmospheric oxygen to water and couples the oxygen reduction reaction to the creation of a membrane proton gradient. The structure of the enzyme has been solved; however, the mechanism of proton pumping is still poorly understood. Recent electrostatic calculations of this group indicate that one of the histidine ligands of enzyme's Cu_B center, His291, may play the role of the pumping element. In the present paper, we use first principles to study models of the catalytic center of CcO, and calculate the pK_a of the His291 residue for both the reduced and oxidized states of the Cu_B center. We used density functional theory to calculate the proton affinity of the δ-nitrogen of His291, and we used the self-consistent reaction field method to calculate the solvation energies. The pK_a of 4-methylimidazole was calculated first to establish the accuracy of our method. For the reaction center, two different models were used. The minimal model contains only the Cu_B center, its histidine ligands, and a water ligand. The extended model consists of the iron porphyrin (ferryloxy state) of Heme a_3, and its axial histidine, in addition to the Cu_B complex. Using the minimal model, we obtained aqueous phase pK_a's for the His291 residue of 9 and 13, with oxidized and reduced Cu_B respectively. The pK_a's are 6.3 and 14.5 using the extended model. When the dielectric constant is set to $\epsilon = 4$ to reflect protein environment, the pK_a with oxidized Cu_B drops to -4.8, whereas with reduced Cu_B it increases slightly to 15.7.

Introduction

Cytochrome *c* oxidase (CcO) is the terminal trans-membrane enzyme of the respiratory electron transport chain of aerobic organisms; it converts atmospheric oxygen into water and couples the oxygen reduction reaction to proton pumping across the membrane.[1−4] The pumping of protons results in the creation of an electrochemical proton gradient which subsequently drives ATP synthesis.[5]

The proton pumping across the membrane must work against both electric and pH gradients. The reduction of O_2 to $2H_2O$ in the catalytic center of the enzyme is recognized to provide energy for the process;[1−4] however, the exact mechanism of the coupling between the redox chemistry and the uphill proton translocation is poorly understood. Much has been learned since the structure of the enzyme was solved,[6,7] but the key residues involved in redox-coupled proton activity still remain unidentified.

Recent electrostatic calculations of this group indicate that one of the histidine ligands of the enzyme's Cu_B center, His291, may play the role of the pumping element.[8,9] The proposed pumping model states that upon reduction of the binuclear center, the His291 ligand picks up a proton from Glu242, an established proton donor[10−12] located closer to the negative side of the membrane, and, upon arrival of another, so-called chemical proton to the binuclear center, releases the first proton toward the positive side of the membrane. Thus, a key element of the model is the dependence of the protonation state of His291 on the redox state of the metal center.

The calculations were based on a semiempirical continuum electrostatic method.[13−20] In this method, starting from experimental data for the pK_a's of model compounds in aqueous solution, the procedure estimates the pK_a's of the protonatable groups in the protein environment by calculating the difference in solvation energy and the effect of electric charges of the protein. The model has been shown to produce reasonable results for proteins when the aqueous pK_a values of the adequately chosen model compounds are known.[21−28]

The choice of the model compound in the electrostatic calculations is critical. It is not always that a protonatable group in the protein would have a suitable analogue in aqueous solution with known pK_a value, as, for example, for the Cu_B center in cytochrome oxidase. In such cases, the aqueous value of the pK_a should be either estimated or independently calculated.[29−32] In our previous work, the aqueous pK_a value of the His291 ligand in the oxidized form of the Cu_B center was estimated to be around 7, for which the calculated data were reported. The main qualitative results were verified to hold for pK_a values in the range 5−11 for the model compound. However, the exact value of the aqueous pK_a value for the His291 ligand was not known.

In the present paper, we use first principles to study the pK_a of the His291 residue for both the reduced and oxidized states of the Cu_B center. We use density functional theory to calculate the proton affinity of the δ-nitrogen of His291, and the self-consistent reaction field method to calculate the solvation energies. The pK_a of 4-methylimidazole was calculated first to establish the accuracy of our method. For the reaction center, two different models were used. The minimal model contains only the Cu_B center, its histidine ligands, and a water ligand. The extended model consists of the iron porphyrin (ferryloxy state) of Heme a_3, and its axial histidine, in addition to the Cu_B complex. Using the minimal model, we obtained aqueous phase pK_a's for the His291 residue of 9 and 13, with oxidized and reduced Cu_B, respectively. The pK_a's are 6.3 and 14.5 using the extended model. When the dielectric constant is set to $\epsilon =$

* Corresponding author. Fax: 530-752-8995. E-mail: stuchebr@chem.ucdavis.edu.

10.1021/jp0467797 CCC: $27.50
Published on Web 11/04/2004

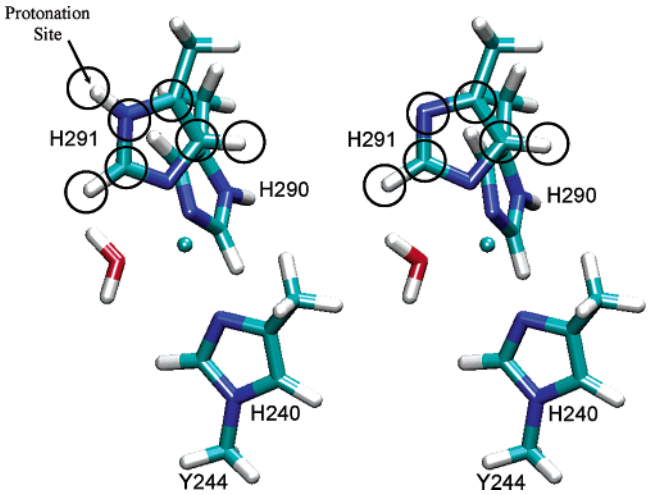

Figure 1. Minimal model of the Cu_B center used to calculate the pK_a of His291. The protonated and deprotonated forms (of His291) are pictured in panels A and B, respectively. Only the circled atoms are allowed to relax during the geometry optimization.

4 to reflect protein environment, the pK_a with oxidized Cu_B drops to −4.8, whereas with reduced Cu_B it increases slightly to 15.7.

A similar electron-coupled pK_a change has been suggested as being responsible for the pH dependent redox potential of the Rieske iron−sulfur protein of cytochrome bc_1 complex.[33−36] In this case, the reaction center consists of two histidines ligated to one of two iron atoms in an iron−sulfur complex. In a recent density functional theory study very similar to the one employed here, Ullmann and co-workers calculated the pK_A of one of the histidines to be 6.9 for the oxidized state of iron, and 11.3 for the reduced state.[32] These values are similar to those estimated from experiments (see ref 36 and references therein).

To evaluate the absolute pK_a value of the His291 residue in the protein, more sophisticated studies are required. In addition to the calculations reported here, the inhomogeneity of the protein dielectric must be take into account, and the effect of the protein charges, which should be found in a self-consistent manner, must also be described adequately. This significant extension of the calculations is described in a companion paper.[37]

Models and Methods

The starting structure of the binuclear center complex was taken from the X-ray crystal structure of bovine heart cytochrome *c* oxidase obtained by Yoshikawa et al, at 2.3 Å resolution (2OCC in the protein data bank).[7] The minimal model (Figure 1) required to calculate the pK_a of a Cu_B ligand consists of the Cu atom, methylimidazole (MeIm) molecules representing coordinated histidines 240, 290, and 291, a methyl group representing tyrosine 244 (which is cross-linked to His240), and an H_2O Cu_B ligand. (Our residue numbering refers to subunit A of bovine CcO enzyme.) The methyl groups attached to the imidazole rings represent the β-methylene groups of histidine. A full description of Tyr244 is not necessary because we are only interested in the acidity of the His291 ligand.

An extended model system (depicted in Figure 2) consists of the Cu_B center discussed above, the Heme a_3 Fe atom and its ligands: an oxygen atom, the porphyrin ring system, and His376. A similar model has been studied in ref 38. Hydrogen atoms replace all eight side groups of the porphyrin, including the farnesyl tail and both propionates. (The effect of the charged

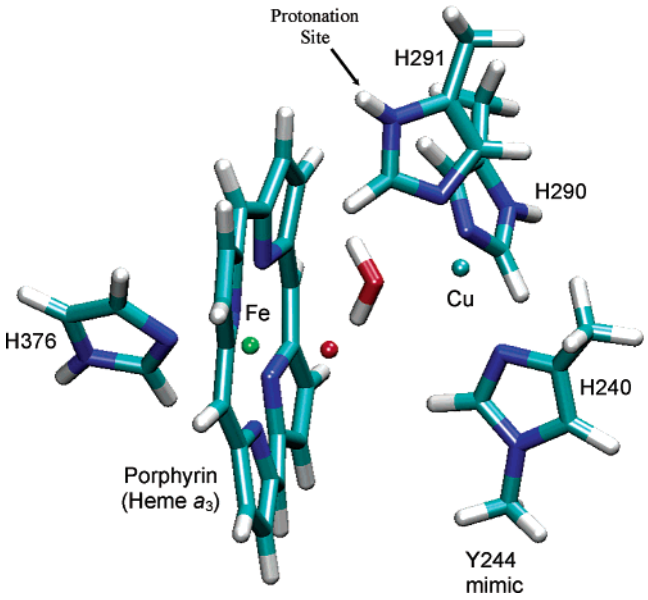

Figure 2. Extended model. The water molecule and the oxygen atom atom ligated to Fe were optimized with the B3LYP/LACVP+* method, in the protonated/reduced state, while all other atoms were kept fixed.

propionates, as well as other charged groups of the protein, is included in a separate electrostatic calculation reported elsewhere, in which the inhomogeneity of the dielectric protein medium is also taken into account, see ref 8 and the companion paper, ref 37). As with the Cu_B ligands, an imidazole represents the His376 residue. The 6-coordinate ferryloxy state $[Fe{=}O]^{+2}$ is expected to be a diradical triplet.[39,40] Though we only report results for the triplet ferryloxy state, we have found it to be more stable than both the singlet and quintet spin states. The overall spin state of the Cu_B−Heme a_3 complex is triplet for Cu^+ (reduced, R) and quartet for Cu^{2+} (oxidized, O). Inclusion of the propionates would serve to stabilize the protonated form of His291; thus the pK_a values that we report here will be underestimated. Future studies will address this issue.

Energies of each coupled protonation/redox state of the complex were calculated using density functional theory (DFT)[41,42] and the Jaguar 5.5 quantum chemistry package.[43] All calculations used the hybrid density functional B3LYP,[44] and open shell electronic configurations were calculated with the restricted open-shell variant of DFT. Reported energies used the LACV3P+* basis set, whereas geometry optimizations used LACVP+*, as abbreviated in the Jaguar program.[43,45] These basis sets include nonrelativistic electron core potentials for the Fe and Cu atoms. The basis sets for the metal valence electrons (and all nonmetal electrons) are of split valence quality (6-31+G* [46−51]) for LACVP+* and triple split valence quality (6-311+G* [52−55]) for LACV3P+*. They include polarization and diffuse functions for all heavy atoms.

Geometry optimizations were conducted in Cartesian space. For the minimal model (Figure 1), the Cu atom, the ligating ϵ-nitrogen, and methyl group of methylimidazole 291 were kept fixed, along with the methylimidazole 290 and dimethylimidazole 240 ligands. This scheme allows relaxation of the remaining atoms while the integrity of the crystal stucture is preserved with respect to both the unique Cu−ligand geometry as well as the attachment location of the histidines to the protein backbone. Four optimizations were performed: for the protonated and deprotonated forms of His291, and each of these for oxidized and reduced Cu_B. The geometry of the Cu-ligated water molecule was set using molecular mechanics. This water

SCHEME 1: Deprotonation of the 4-Methylimidazole Molecule

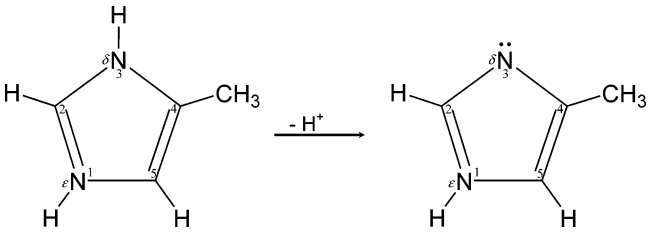

molecule is known to be very weakly bound and quite mobile.[56,57] Indeed, its location has very little affect on the pK_a of His291. For the extended model system, these same Cu_B complex geometries were used. In addition, the H_2O and ferryloxy oxygen ligands were optimized only for oxidized copper, keeping all other atoms (including the metal atoms) fixed.

To quantify the effect of solvation, the complex was surrounded by a continuum dielectric (either $\epsilon = 80$ or $\epsilon = 4$) and the free energy of solvation (G_{solv}) calculated using the self-consistent reaction field (SCRF) method as implemented in Jaguar 5.5.[58,59] The solvation free energy is written as a sum of the electronic reorganization of the solute, G_{solv}^{reorg}, the electrostatic interaction of the solute with the induced polarization of the surrounding dielectric, $G_{solv}^{solvent}$, plus the work required to create the solvent cavity, G_{solv}^{cav}:

$$G_{solv} = G_{solv}^{reorg} + G_{solv}^{solvent} + G_{solv}^{cav} \quad (1)$$

The cavity term is not included in our studies because it has a negligible effect on the pK_a. The size and shape of the cavity change very little with complete deprotonation. The probe radius of the surrounding dielectric was set to 1.4 Å, the standard for aqueous solvation.[43]

Results and Discussion

Calculation of 4-Methylimidazole pK_a. To establish a benchmark for the accuracy of our pK_a predictions, we calculated the absolute pK_a for both the δ- and ϵ-nitrogen sites of 4-methylimidazole (MeIm; see Scheme 1). The pK_a is written

$$pK_a = \frac{1}{kT \ln 10} \Delta G_{dissoc}^{aq} \quad (2)$$

The free energy of proton dissociation in water, ΔG_{dissoc}^{aq}, can be predicted using the thermodynamic cycle depicted in Figure 3. Here we faithfully follow the calculation method described by Noodleman and co-workers.[32,60] Accordingly, eq 2 is expanded to give

$$pK_a = \frac{1}{kT \ln 10} [\Delta G_{dissoc}^{vac} + (G_{solv}^{deprot} + G_{solv}^{H^+} - G_{solv}^{prot})] \quad (3)$$

The first term, the free energy of proton dissociation in a vacuum, can be expressed as

$$\Delta G_{dissoc}^{vac} = \Delta E^{elec} + \Delta E^{vib} + \Delta E^{trans} + \Delta(pV) - T\Delta S \quad (4)$$

From left to right, the terms in eq 4 denote the electronic and the zero point vibrational energy differences between the deprotonated and protonated species, the energy of proton ejection, the energy due to the gas phase volume change, and finally the entropy contribution. To calculate the absolute pK_a of MeIm, we used the B3LYP functional and the 6-311+G* basis set for optimizations, energy calculations as well as the calculation of the zero point energy. Our results and our approximations are summarized in detail in Table 2. We obtain values of 7.7 and 7.8 for the δ and ϵ pK_a values, respectively (compared with established experimental values 6.6 and 7.0 for histidine).[61]

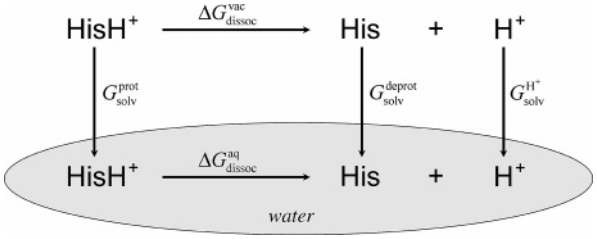

Figure 3. Thermodynamic cycle describing the standard technique for calculating the free energy of proton dissociation in aqueous solution, ΔG_{dissoc}^{aq}, needed here to calculate the pK_a of doubly protonated histidine ($HisH^+$; see Scheme 1). The free energy of dissociation in a vacuum must be calculated accurately, and the solvation free energies (G_{solv}) of $HisH^+$ and His must be obtained on an equal footing. The solvation free energy of a proton (H^+) in water is known from experiment.[66]

TABLE 1: Proton Affinity (PA) of 4-Methylimadazole at the 3-Position (δ-Nitrogen in Histidine, Scheme 1)[a]

method	PA	ref
PHP MS[b]	224.8	67
FT-ICR MS[c]	226.2	68
MP2/TZ2P//HF/DZP[d]	227.0	68, 69
MP2/6-311+G* [e]	223.9	this work
B3LYP/6-311+G* [f]	227.0	this work

[a] Results from this work calculated using both DFT and MP2 Are compared with previous values from theory and experiment. For all three theoretical predictions, the zero point energy was calculated using the same method and basis set used for geometry optimization. The DFT (B3LYP) result was used to calculate the pK_a of MeIm (Table 2). [b] Pulsed High-Pressure Mass Spectrometry. [c] Fourier Transform Ion Cyclotron Resonance Mass Spectrometry. [d] Triple-ζ plus double polarization;[70,71] double-ζ plus polarization.[70,72] [e] MP2/6-311+G*//MP2/6-311+G*, with local MP2 method implemented in Jaguar. [f] Reference system: B3LYP/6-311+G*//B3LYP/6-311+G*.

In addition to the pK_a, the enthalpy of proton affinity is an experimentally measurable quantity with which we may compare our results. It is a measure of the accuracy of our results in a vacuum instead of solution and therefore does not include the added complication of solvation energies. The proton affinity is defined as $-\Delta H_r$ for the reaction $B + H^+ \rightarrow BH^+$ and is therefore written[62]

$$PA = \Delta H_{dissoc}^{vac} = \Delta E^{elec} + \Delta E^{vib} + {}^5/_2 kT \quad (5)$$

where the change in vibrational energy during heating from 0 to 298 K has been neglected. Values for the proton affinity of the nitrogen at the 3-position in 4-methylimidazole obtained from theory and experiment are compared in Table 1. The proton affinity that we calculate (227.0 kcal/mol) compares well to the most recent experimental value (226.2 kcal/mol). As a result, we feel confident that we can accurately calculate the pK_a of His291 in the Cu_B complex.

Calculation of His291 pK_a. Though our method predicts the δ pK_a of our reference compound within 1.1 pK_a units of the experimental value, we expect to achieve much better accuracy when we compare pK_a's that are obtained in a similar manner. Consequently, our strategy for quantifying the pK_a of the His291

TABLE 2: Absolute pK_a of a Reference System and a Test of the Method[a] [Results for the δ- and ϵ-Nitrogen pK_a's of Methylimidazole (Scheme 1)]

	4-methylimidazole (His mimic)	
	δ-N site	ϵ-N site
ΔG^{vac}_{dissoc} (a)	219.2	219.7
ΔE_{elec}	234.6	235.0
ΔE_{vib}	−9.0	−8.9
ΔE_{trans}, $^3/_2 k_B T$	0.9	0.9
$\Delta(pV)$, $k_B T$	0.6	0.6
$-\Delta(T\Delta S)$	−7.8	−7.8
$G^{prot}_{solv}(HisH^+)$ (b)	−64.6	−64.6
G^{reorg}_{solv} ("strain" energy)	1.5	1.5
$G^{solvent}_{solv}$ (Born energy)	−66.1	−66.1
G^{deprot}_{solv} (His) (c)	−12.8	−13.2
G^{reorg}_{solv}	4.0	4.8
$G^{solvent}_{solv}$	−16.8	−17.9
$G^{H^+}_{solv}(H^+)$ (experimental[66])	−260.5	−260.5
ΔG^{aq}_{dissoc} (a − b + c + d)	10.5	10.7
pK_a	7.7	7.8
pK_a (experimental[61])	6.6	7.0

[a] The translational energy of a proton is $^3/_2 k_B T$, and the value for the volume change is taken from the ideal gas equation to be $k_B T$. The entropic contribution, $\Delta(T\Delta S)$, was set to 7.8 kcal/mol, as derived from the Sekhur−Tetrode equation.[32,73] Energies are calculated using the B3LYP DFT functional with the LACV3P+* basis set, and are reported in kcal/mol. Free energies of solvation for both the protonated and deprotonated species were calculated using the DFT/SCRF method. Zero point vibrational energies were calculated with the harmonic approximation, and the frequencies were left unscaled.

Cu_B ligand is to simply subtract off the error in our calculation of the pK_a for the reference compound

$$\begin{aligned} \mathrm{p}K_a(\mathrm{H291}) &= \mathrm{p}K_a^{calc}(\mathrm{H291}) - \text{error} \\ &= \mathrm{p}K_a^{calc}(\mathrm{H291}) - (\mathrm{p}K_a^{calc}(\mathrm{MeIm}) - \mathrm{p}K_a^{exp}(\text{histidine})) \\ &= \Delta'\mathrm{p}K_a^{calc}(\mathrm{H291} - \mathrm{MeIm}) + 6.6 \end{aligned} \quad (6)$$

As indicated, Δ' signifies the differencing of values for His291 and MeIm. Equation 6 shows that we do not need to calculate the pK_a of either His291 or the reference compound, but rather the pK_a shift only.

The shift in the pK_a of Cu-ligated His291 from that of methylimidazole is obtained straightforwardly from eq 3:

$$\Delta'\mathrm{p}K_a^{calc} = \frac{1}{kT\ln 10}[\Delta'\Delta G^{vac}_{dissoc} + (\Delta' G^{deprot}_{solv} + \Delta' G_{solv}{}^{H^+} - \Delta' G^{prot}_{solv})] \quad (7)$$

The term $\Delta' G^{H^+}_{solv}$ in eq 7 is trivially zero. Moreover, the final four terms in the expansion of ΔG^{vac}_{dissoc} in eq 4 can be considered the same for deprotonation of His291 ligated to Cu_B and the reference compound, 4-methylimidazole. Hence, the difference in the gas-phase free energies of proton dissociation between His291−Cu_B and MeIm can be approximated by the quantity of which we are most confident, the difference in the electronic energies of reaction,

$$\Delta'\Delta G^{vac}_{dissoc} \simeq \Delta'\Delta E^{elec}_{dissoc} \quad (8)$$

TABLE 3: Results for the Gas Phase Electronic Energy of δ-Proton Ionization, ΔE^{elec}_{dissoc}, for Methylimidazole (MeIm) and His291 Ligated to Oxidized and Reduced Cu_B[a]

compound	ΔE^{elec}_{dissoc}	$\Delta'\Delta E^{elec}_{dissoc}$
MeIm	234.6	0
minimal model		
H291−Cu^{1+} (R)	283.7	49.1
H291−Cu^{2+} (O)	198.7	−35.9
extended model		
H291−Cu^{1+} (R)	292.5	57.9
H291−Cu^{2+} (O)	218.0	−16.6

[a] Energies are calculated using the B3LYP DFT functional with the LACV3P+* basis set and are reported in kcal/mol. Δ' marks the difference, H291 − MeIm.

The pK_a shift (eq 7) is now expressed more simply as

$$\Delta'\mathrm{p}K_a^{calc} = \frac{1}{kT\ln 10}(\Delta'\Delta E_{elec} + \Delta'\Delta G_{solv}) \quad (9)$$

Inserting eq 9 into eq 6 gives an accurate prescription for the pK_a of His291 protonation site of the Cu_B complex in aqueous solution:

$$\mathrm{p}K_a = \frac{1}{kT\ln 10}(\Delta'\Delta E_{elec} + \Delta'\Delta G_{solv}) + 6.6 \quad (10)$$

Table 3 summarizes our results for the proton dissociation in a vacuum, ΔE_{elec}, of both the reference compound as well as His291 ligated to Cu_B using the minimal and extended models, respectively.

The calculated solvation free energies are presented in Table 4. Two different models, the minimal model (Figure 1), and the extended model (Figure 2), were used in the calculations. Unfortunately, there are no corresponding experimental measurements with which to compare our results and to estimate the accuracy of the obtained salvation energies. To get a sense of the magnitude of the error in such calculations, we report here results obtained with two different methods for evaluation of the solvation energy. For the minimal model, both the DFT/SCRF method as implemented in Jaguar, and the reaction field (RF) method using the Solvate program of the MEAD suite[13,63,64] were used. For the extended model, only the DFT/SCRF method was used.

It is instructive to compare results of our calculations with the predictions of a simple Born model.[65] In this model, the polarization energy of the solvent is equal to the work required to transfer an ion from vacuum to a spherical solvent cavity of radius a,

$$G^{elec}_{solv} = -\frac{q^2}{2a}\left(1 - \frac{1}{\epsilon}\right) \quad (11)$$

where q is the charge of the ion and ϵ is the dielectric constant of the medium. Because the deprotonation of His291 in the oxidized state causes the total charge to decrease from +2 to +1 but the effective radius to remain roughly unchanged, one can expect the solvation energy to decrease by a factor of 4. Our studies yield a decrease by a factor of ∼3 using the minimal model and by 2.4 using the extended model. The difference between our calculated ratio and the Born model prediction is due to reorganization of charge (see Figures 4 and 5) in our nonspherical and electronically nonuniform solute. Comparing the two redox states of the Cu atom, the protonated-His291/reduced-Cu_B and deprotonated-His291/oxidized-Cu_B systems both have the same total charge (+1), so one should expect

TABLE 4: Calculations of the Free Energy of Solvation (in $\epsilon = 80$) for the δ-Deprotonated and Protonated Forms of MeIm and His291 Ligated to Cu_B, Using Both the Minimal Model and the Extended Model[a]

	protonated			deprotonated				
compound	G_{solv}^{reorg}	$G_{solv}^{solvent}$	G_{solv}	G_{solv}^{reorg}	$G_{solv}^{solvent}$	G_{solv}	ΔG_{solv}	$\Delta'\Delta G_{solv}$
SCRF/minimal								
MeIm	1.5	−66.1	−64.6	4.0	−16.8	−12.8	51.8	0
H291−Cu^{1+} (R)	3.3	−55.6	−52.3	9.4	−49.5	−40.1	12.2	−39.6
H291−Cu^{2+} (O)	3.7	−160.8	−157.1	10.2	−76.4	−66.1	90.9	39.1
RF/minimal								
MeIm	1.5	−64.4	−62.9	4.0	−12.2	−8.2	54.7	0
H291−Cu^{1+} (R)	3.3	−59.2	−55.9	9.4	−50.7	−41.3	14.6	−40.1
H291−Cu^{2+} (O)	3.7	−165.3	−161.6	10.2	−78.9	−68.7	92.9	38.2
SCRF/extended								
MeIm	1.5	−66.1	−64.6	4.0	−16.8	−12.8	51.8	0
H291−Cu^{1+} (R)	6.7	−64.7	−58.1	12.4	−65.5	−53.1	5.0	−46.8
H291−Cu^{2+} (O)	4.8	−138.2	−133.4	7.8	−73.0	−65.2	68.2	16.4

[a] Calculations for the minimal model were carried with both the self consistent reaction field (SCRF) method and the jaguar program, and with the reaction field (RF) method using the solvate program of the MEAD suite. Calculations for the extended model were done only with the SCRF method. The difference in solvation between the deprotonated and protonated species is defined as, $\Delta G_{solv} = G_{solv}^{deprot} - G_{solv}^{prot}$, and Δ' marks the difference, H291 − MeIm. Energies are reported in kcal/mol.

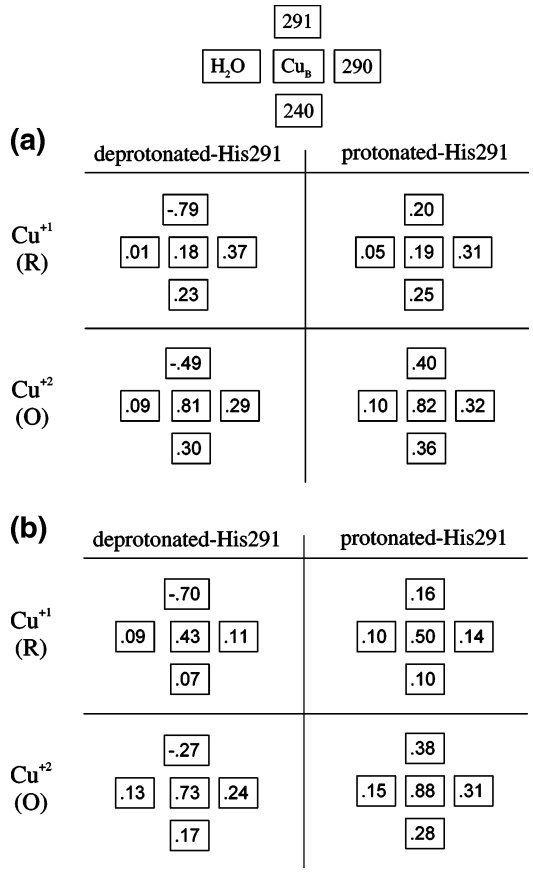

Figure 4. (a) Electrostatic potential of the Cu_B complex (Figure 1) in a dielectric continuum of $\epsilon = 80$, calculated using B3LYP/LACV3P+*. Charges were obtained by the SCRF method the electrostatic potential fitting procedure implemented in the Jaguar program.[43] They are summed for each ligand with the atomic charge for Cu_B presented in the center (see the key at the top, where histidine ligands are marked only with their residue number. (b) Mullekin charges of the Cu_B complex (Figure 1) in a vacuum, calculated using B3LYP/LACV3P+*. They are summed for each ligand with the atomic charge for Cu_B presented in the center (see the key at the top, where histidine ligands are marked only with their residue number.

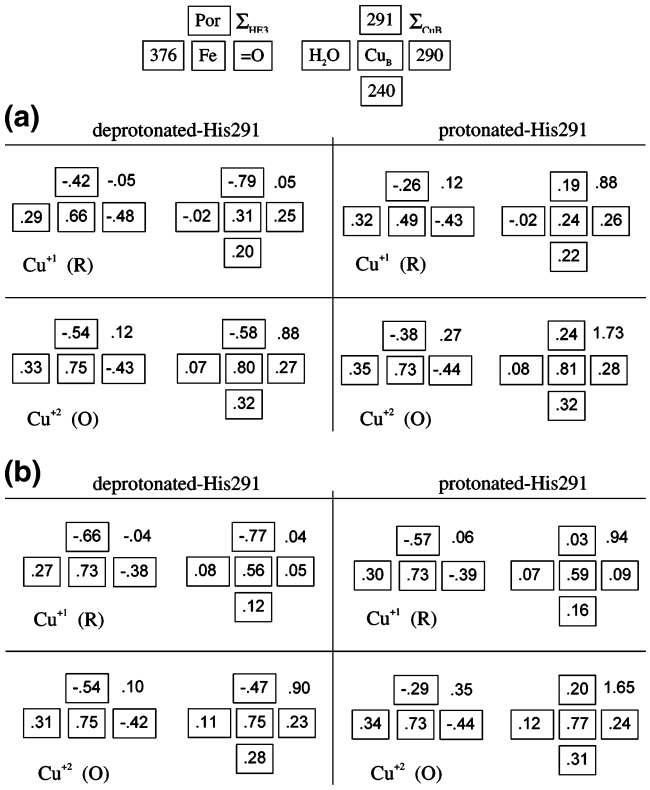

Figure 5. (a) Electrostatic potential of the FePor/Cu_B complex (Figure 2) in a dielectric continuum of $\epsilon = 80$. Charges are calculated and presented just as those of Figure 4a (see key at top for description). The numbers not surrounded by a box are the total charges of Heme a_3 center and the Cu_B complex. (b) Mullekin charges of the FePor/Cu_B complex (Figure 2) in a vacuum using the extended model. Charges are calculated and presented just as those of Figure 4b (see key at top for description). The numbers not surrounded by a box are the total charges of Heme a_3 center and the Cu_B complex.

them to have similar solvation energies. The exact calculations predict the solvation energy of the oxidized species to be a factor of ∼1.2 larger than that of the reduced species. This is due to greater charge separation in the oxidized-deprotonated state than in the reduced-protonated state (Figures 4 and 5).

Table 5 lists the different energy terms of the aqueous pK_a calculations, and Table 6 shows final results for the obtained pK_a values of the His291 Cu_B ligand. In aqueous solution, depending on the model, in the reduced state of Cu_B center, the pK_a of His291 varies in the range of 13.5 to 14.5, whereas in the oxidized state, the pK_a is found to be in the range of 6.3 to 9.3.

The protein environment will significantly change these values, due to different dielectric properties of the protein

TABLE 5: Calculation of the ΔpK_a (Eq 9) of His291 for Oxidized and Reduced Cu_B with Solvation Energies Calculated Using Either the SCRF Method and the Jaguar Program (for Both the Minimal and Extended Models) or the Reaction Field (RF) Method with the Solvate Program of the MEAD Suite[a]

	reduced Cu_B			oxidized Cu_B		
	SCRF/min	RF/min	SCRF/ext	SCRF/min	RF/min	SCRF/ext
$\Delta'\Delta E^{elec}_{dissoc}$ (a)	49.1	49.1	57.9	−35.9	−35.9	−16.7
$\Delta'G^{deprot}_{solv}$ (b)	−27.5	−33.0	−40.3	−52.9	−60.0	−52.4
$\Delta'G^{prot}_{solv}$ (c)	12.2	7.0	6.5	−92.5	−98.7	−68.8
$\Delta'\Delta G^{aq}_{dissoc}$ (a + b − c)	9.4	9.1	11.1	3.7	2.8	−0.3
$\Delta' pK_a^{calc}$	6.7	6.6	7.9	2.7	2.0	−0.3

[a] DFT energies are calculated using B3LYP/LACV3P+*. Δ' marks the difference, His291 − MeIm. Energies are given in kcal/mol,

TABLE 6: Theoretical Estimates for the pK_a of His291 for the Reduced and Oxidized States of Cu_B, Calculated According to Eq 10 and Table 4[a]

method	reduced Cu_B	oxidized Cu_B
$\epsilon = 80$		
SCRF/min	13.5	9.3
RF/min	13.2	8.6
SCRF/ext	14.5	6.3
$\epsilon = 4$		
SCRF/min	13.2	−5.0
RF/min	9.8	−9.9
SCRF/ext	15.7	−4.8

[a] The difference in pK_a between the oxidized and reduced states of Cu_B suggests that oxidation would result in the release of a proton from His291.

medium and the effect of protein charges. It is these changes that the electrostatic calculations of ref 8 intend to evaluate. In the reported earlier work, the aqueous pK_a value of His291 in the oxidized state of Cu_B was estimated to be around 7, and the proposed pumping scheme was verified to hold for pK_a values in the range of 5 to 11. The present calculation supports our earlier ad hoc estimate.

For comparison purposes, the described calculations were repeated in a uniform medium with dielectric constant $\epsilon = 4$, characteristic for proteins. The results are listed in Table 6. The details of the calculations are given in the Supporting Information. In the reduced state of the complex, the pK_a of His291 is found to be well above 7, whereas in the oxidized state, with increased positive charge of the metal, the pK_a drops to negative values. Such a dependence shows that already in a low dielectric medium, the protonation state of the Cu_B center should be expected to depend on its redox state. This redox dependence is one of the key ingredients of the Coulomb pumping model described in refs 8 and 9.

The real protein is more complicated because the dielectric medium is not uniform and because surrounding protein charges significantly affect the energetics of protonation. Moreover, to work as a pumping element, and to relay protons along the proton conducting chain, the redox-dependent pK_a values of His291 should be compared with pK_a's of the corresponding donor and acceptor groups in the chain. These questions require significant extension of the described calculations, and are examined in a separate paper.[37]

Conclusions

We used density functional theory to calculate the proton affinity and the solvation energy of 4-methylimidazole using the B3LYP functional and the 6-311+G* basis set. We obtain the δ pK_a of 4-MeIm to within 1.1 units of the established experimental value. Using this as a measure of the error of our results, we calculated the pK_a of two models of the Cu_B center in cytochrome oxidase, as a function of the redox state of the Cu atom. In the oxidized state, the found aqueous pK_a value is in the range 6.3−9.3. This information agrees with the ad hoc estimate of 7 used in our earlier electrostatic calculations and support the proposed His291 proton pumping model of cytochrome oxidase.[8,9]

Inclusion of propionates A and D of Heme a_3 in the calculation, as well as other protein charged groups, along with the effects of inhomogeneity of the protein dielectric, will be presented in a forthcoming publication. The possibility that His290, another ligand of the Cu_B atom, serves as the proton loading site for subsequent pumping is an issue that must also be examined. When protonated, the δ-nitrogen of His290 is hydrogen bonded to threonine 305. As a result, deprotonation of His290 is significantly hindered. In a future publication, we will address this issue by calculating deprotonation energies in the presence of the surrounding charges of the enzyme.

Acknowledgment. We thank Xuehe Zheng for his helpful input. This work has been supported by the NSF and a research grant from the NIH (GM54052).

Supporting Information Available: Cartesian coordinates for the extended model: both the deprotonated and protonated forms of His291. Solvation free energies using the SCRF and the Jaguar program or the RF method and the Mead program in dielectric continuum of $\epsilon = 4$. This material is available free of charge via the Internet at http://pubs.acs.org.

References and Notes

(1) Wikström, M. *Nature* **1977**, *266*, 271.
(2) Wikström, M. *Curr. Op. Struct. Biol.* **1998**, *8*, 480.
(3) Michel, H.; Behr, J.; Harrenga, A.; Kannt, A. *Annu. Rev. Biopys. Biomol. Struct.* **1998**, *27*, 329.
(4) Gennis, R. B. *Proc. Natl. Acad. Sci. U.S.A.* **1998**, *95*, 12747.
(5) Mitchell, P. *Nature* **1961**, *191*, 144.
(6) Iwata, S.; Ostermeier, C.; Ludwig, B.; Michel, H. *Nature* **1995**, *376*, 660.
(7) Yoshikawa, S.; Shinzawa-Itoh, K.; Nakashima, R.; Yaono, R.; Yamashita, E.; Inoue, N.; Yao, M.; Fei, M. J.; Libeu, C. P.; Mizushima, T.; Yamaguchi, H.; Tomizaki, T.; Tsukihara, T. *Science* **1998**, *280*.
(8) Popović, D. M.; Stuchebrukhov, A. A. *J. Am. Chem. Soc.* **2004**, *126*, 1858.
(9) Popović, D. M.; Stuchebrukhov, A. A. *FEBS Lett.* **2004**, *566*, 126.
(10) Ädelroth, P.; Svensson Ek, M.; Mitchell, D. M.; Gennis, R. B.; Brzezinski, P. *Biochemistry* **1997**, *36*, 13824.
(11) Verkhovskaya, M. L.; Garcia-Horsman, A.; Puustinen, A.; Rigaud, J.-L.; Morgan, J. E.; Verkhovsky, M. I.; Wikström, M. *Proc. Natl. Acad. Sci. U.S.A.* **1997**, *94*, 10128.
(12) Zaslavsky, D.; Sadoski, R. C.; Rajagukguk, S.; Geren, L.; Millett, F.; Durham, B.; Gennis, R. B. *Proc. Natl. Acad. Sci. U.S.A.* **2004**, *101*, 10544.
(13) Bashford, D.; Karplus, M. *Biochemistry* **1990**, *29*, 10219.
(14) Bashford, D.; Karplus, M. *J. Phys. Chem.* **1991**, *95*, 9557.
(15) Beroza, P.; Fredkin, D. R.; Okamura, M. Y.; Feher, G. *Proc. Natl. Acad. Sci. U.S.A.* **1991**, *88*, 5804.
(16) Gunner, M. R.; Honig, B. *Proc. Natl. Acad. Sci. U.S.A.* **1991**, *88*, 9151.
(17) Yang, A.-S.; Gunner, M. R.; Sompogna, R.; Honig, B. *Prot. Struct. Funct. Genet.* **1993**, *15*, 252.
(18) Beroza, P.; Case, D. A. *J. Phys. Chem.* **1996**, *100*, 20156.
(19) Ullmann, G. M.; Knapp, E. W. *Eur. Biophys. J.* **1999**, *28*, 533.
(20) Baptista, A. M.; Martel, P. J.; Soares, C. M. *Biophys. J.* **1999**, *76*, 2978.
(21) Sampogna, R. V.; Honig, B. *Biophys. J.* **1994**, *66*, 1341.
(22) Gunner, M. R.; Nicholls, A.; Honig, B. *J. Phys. Chem.* **1996**, *100*, 4277.
(23) Lancaster, C. R.; Michel, H.; Honig, B.; Gunner, M. R. *Biophys. J.* **1996**, *70*, 2469.

(24) Kannt, A.; Lancaster, R. D.; Michel, H. *Biophys. J.* **1998**, *74*, 708.
(25) Rabenstein, B.; Ullmann, G. M.; Knapp, E. W. *Biochemistry* **1998**, *37*, 2488.
(26) Popović, D. M.; Zaric, S. D.; Rabenstein, B.; Knapp, E. W. *J. Am. Chem. Soc.* **2001**, *123*, 6040.
(27) Spassov, V. Z.; Luecke, H.; Gerwert, K.; Bashford, D. *J. Mol. Biol.* **2001**, *312*, 203.
(28) Popović, D. M.; Zmiric, A.; Zaric, S. D.; Knapp, E. W. *J. Am. Chem. Soc.* **2002**, *124*, 3775.
(29) Mouesca, J. M.; Chen, J. L.; Noodleman, L.; Bashford, D.; Case, D. A. *J. Am. Chem. Soc.* **1994**, *116*, 11898.
(30) Kallies, B.; Mitzner, R. *J. Phys. Chem. B* **1997**, *101*, 2959.
(31) Richardson, W. H.; Peng, C.; Bashford, D.; Noodleman, L.; Case, D. A. *Int. J. Quantum Chem.* **1997**, *61*, 207.
(32) Ullmann, G. M.; Noodleman, L.; Case, D. A. *J. Biol. Inorg. Chem.* **2002**, *7*, 632.
(33) Prince, R. C.; Dutton, P. L. *FEBS Lett.* **1976**, *65*, 117.
(34) Link, T. A.; Hagen, W. R.; Pierik, A. J.; Assmann, C.; von Jagow, G. *Eur. J. Biochem.* **1992**, *208*, 685.
(35) Kuila, D.; Schoonover, J.; FDyer, R. B.; Batie, C. J.; Ballou, D. P.; Fee, J. A.; Woodruff, W. H. *Biochim. Biophys. Acta* **1992**, *1140*, 175.
(36) Baymann, F.; Robertson, D. E.; Dutton, P. L.; Mäntele, W. *Biochemistry* **1999**, *38*, 13188.
(37) Popović, D. M.; Quenneville, J.; Stuchebrukhov, A. A. Manuscript in preparation.
(38) Moore, D. B.; Martínez, T. J. *J. Phys. Chem. A* **2000**, *104*, 2367.
(39) Green, M. T. *J. Am. Chem. Soc.* **2000**, *122*, 9495.
(40) Green, M. T. *J. Am. Chem. Soc.* **2001**, *123*, 9218.
(41) Hohenberg, P.; Kohn, W. *Phys. Rev.* **1964**, *136*, B864.
(42) Kohn, K.; Sham, L. J. *Phys. Rev.* **1965**, *140*, A1133.
(43) Jaguar 5.5, S., L.L.C., Portland, OR, 1991−2003.
(44) Becke, A. D. *J. Chem. Phys.* **1993**, *98*, 5648.
(45) Hay, P. J.; Wadt, W. R. *J. Chem. Phys.* **1985**, *82*, 299.
(46) Ditchfield, R.; Hehre, W. J.; Pople, J. A. *J. Chem. Phys.* **1971**, *54*, 724.
(47) Hehre, W. J.; Pople, J. A. *J. Chem. Phys.* **1972**, *56*, 4233.
(48) Hehre, W. J.; Ditchfield, R.; Pople, J. A. *J. Chem. Phys.* **1972**, *56*, 2257.
(49) Binkley, J. S.; Pople, J. A. *J. Chem. Phys.* **1977**, *66*, 879.
(50) Hariharan, P. C.; Pople, J. A. *Theor. Chim. Acta* **1973**, *28*, 213.
(51) Francl, M. M.; W. J. Pietro; Hehre, W. J.; Binkley, J. S.; Gordon, M. S.; DeFrees, D. J.; Pople, J. A. *J. Chem. Phys.* **1982**, *77*, 3654.
(52) Clark, T.; Chandrasekhar, J.; Spitznagel, G. W.; Schleyer, P. v. R. *J. Comput. Chem.* **1983**, *4*, 294.
(53) Frisch, M. J.; Pople, J. A.; Binkley, J. S. *J. Chem. Phys.* **1984**, *80*, 3265.
(54) Krishnan, R.; Binkley, J. S.; Seeger, R.; Pople, J. A. *J. Chem. Phys.* **1980**, *72*, 650.
(55) McLean, A. D.; S. Chandler, G. *J. Chem. Phys.* **1980**, *72*, 5639.
(56) Blomberg, M. R. A.; Siegbahn, P. E. M.; Babcock, G. T.; Wikström, M. *J. Am. Chem. Soc.* **2000**, *122*, 12848.
(57) Siegbahn, P. E. M.; Blomberg, M. R. A.; Blomberg, M. L. *J. Phys. Chem. B* **2003**, *107*, 10946.
(58) Tannor, D. J.; Marten, B.; Murphy, R.; Friesner, R. A.; Sitkoff, D.; Nicholls, A.; Ringnalda, M. G., W. A., III; Honig, B. *J. Am. Chem. Soc.* **1994**, *116*, 11875.
(59) Marten, B.; Kim, K.; Cortis, C.; Friesner, R. A.; Murphy, R. B.; Ringnalda, M. N.; Sitkoff, D.; Honig, B. *J. Phys. Chem.* **1996**, *100*, 11775.
(60) Li, J.; Nelson, M. R.; Peng, C. Y.; Bashford, D.; Noodleman, L. *J. Phys. Chem. A* **1998**, *102*, 6311.
(61) Tanokura, M. *Biochim Biophys Acta* **1983**, *742*, 576.
(62) Del Bene, J. E.; Metter, H. D.; Frisch, M. J.; Luke, B. J.; Pople, J. A. *J. Phys. Chem.* **1983**, *87*, 3279.
(63) Bashford, D.; Gerwert, K. *J. Mol. Biol.* **1992**, *224*, 473.
(64) Bashford, D. An object-oriented programming suite for electrostatic effects in biological molecules. In *Scientific Computing in Object-Oriented Parallel Environments*; Ishikawa, Y., Oldehoeft, R. R., Reynders, J. V. W., Tholburn, M., Eds.; Springer: Berlin, 1997; Vol. 1343, p 233.
(65) Born, M. *Z. Phys.* **1920**, *1*, 45.
(66) Reiss, H.; Heller, A. *J. Phys. Chem.* **1985**, *89*, 4207.
(67) Meot-Ner, M.; Liebman, J. F.; Bene, J. E. D. *J. Org. Chem.* **1986**, *51*, 1105.
(68) Catalán, J.; Paz, J. L. G. d.; Yáñez, M.; Claramunt, R. M.; López, C.; Elguero, J.; Anvia, F.; Quian, J. H.; Taagepera, M.; Taft, R. W. *J. Am. Chem. Soc.* **1990**, *112*, 1303.
(69) Bliznyuk, A. A.; III, H. F. S.; Amster, I. J. *J. Am. Chem. Soc.* **1993**, *115*, 5149.
(70) Huzinaga, S. *J. Chem. Phys.* **1965**, *42*, 1993.
(71) Dunning, T. H. *J. Chem. Phys.* **1971**, *55*, 716.
(72) Dunning, T. H. *J. Chem. Phys.* **1970**, *53*, 2823.
(73) Hill, T. L. *An introduction to statistical thermodynamics*; Dover: New York, 1960.